Optimal Control and Cost Effectiveness Analysis of SIRS Malaria Disease Model with Temperature Variability Factor

Temesgen Duressa Keno[1,*], Oluwole Daniel Makinde[2] & Legesse Lemecha Obsu[1]

[1]Department of Mathematics, Adama Science and Technology University, Adama, Ethiopia.
[2]Faculty of Military Science, Stellenbosch University, Stellenbosch, South Africa.
*E-mail: temesgenduressaa@gmail.com

Abstract. In this study, we proposed and analyzed the optimal control and cost-effectiveness strategies for malaria epidemics model with impact of temperature variability. Temperature variability strongly determines the transmission of malaria. Firstly, we proved that all solutions of the model are positive and bounded within a certain set with initial conditions. Using the next-generation matrix method, the basic reproductive number at the present malaria-free equilibrium point was computed. The local stability and global stability of the malaria-free equilibrium were depicted applying the Jacobian matrix and Lyapunov function respectively when the basic reproductive number is smaller than one. However, the positive endemic equilibrium occurs when the basic reproductive number is greater than unity. A sensitivity analysis of the parameters was conducted; the model showed forward and backward bifurcation. Secondly, using Pontryagin's maximum principle, optimal control interventions for malaria disease reduction are described involving three control measures, namely use of insecticide-treated bed nets, treatment of infected humans using anti-malarial drugs, and indoor residual insecticide spraying. An analysis of cost-effectiveness was also conducted. Finally, based on the simulation of different control strategies, the combination of treatment of infected humans and insecticide spraying was proved to be the most efficient and least costly strategy to eradicate the disease.

Keywords**:** *cost-effectiveness analysis; malaria disease; optimal control; SIRS model; temperature variability.*

1 Introduction

Malaria is a life-threatening disease caused by a protozoan pathogen. The parasite is known as plasmodium and is transmitted to humans by Anopheles mosquitoes. The parasite can enter the human body when an infected female mosquito in search of a meal bites a susceptible person. For 2018, 228 million cases and 405,000 deaths have been reported globally; the African region accounts for 93% of all cases according to the latest world malaria report from December 2019 [1].

Received December 19th, 2020, Revised April 2nd, 2021, Accepted for publication April 16th, 2021
Copyright © 2020 Published by ITB Institute for Research and Community Services, ISSN: 2337-5760, DOI: 10.5614/j.math.fund.sci.2021.53.1.10

The three main vectors that transmit malaria in tropical Africa are Anopheles gambiae, Anopheles arabiensis and Anopheles funestus [2]. Temperature variability strongly determines the ability of mosquitoes to transmit the disease through the population effectively. It is highest within the range of 16 °C to 28 °C, which creates conditions that are favorable to the breeding rate of mosquitoes [3]. The most common strategies to eradicate malaria are using insecticide-treated bed nets, treatment of infected humans with anti-malarial drugs, and indoor residual insecticide spraying [4].

Mathematical modeling of the transmission of malaria parasites was started by Ronald Ross [5]. He developed an SIS-SI model for human and malaria populations. According to Ross, the number of mosquitoes should be reduced to below a certain threshold to control malaria. Later, several models based on Ross's work have been proposed by scholars who extended his model by considering various impacts such as the existing period of infection (exposure time) for humans and mosquitoes [6-8] and the role of temperature variability on the death rate and birth rate of mosquitoes [9-11].

A number of scholars have formulated malaria models as an optimal control problem to assess the impact of control measures on disease transmission. For instance, Olaniyi *et al.* [12] investigated a malaria model of the spread of the disease with optimal control and conducted an analysis of cost-effectiveness using three control measures. The authors suggest that a combination of using bed nets, treatment with drugs and insecticide spraying is the most efficient and least costly intervention strategy. Makinde & Okosun [13] presented a transmission model for malaria with optimal control using three controls. The authors concluded that the most effective strategies to control malaria transmission are a combination of screening, treatment of infected humans with anti-malarial drugs and indoor insecticide spraying. Okosun *et al.* [14] proposed the SEIRS-SEI model for malaria transmission with optimal control and analysis of cost-effectiveness, applying combinations of three malaria-control measures, i.e. using treated bed nets, treatment of infected humans with drugs and spraying of indoor insecticide. They stated that the most cost-effective controls to prevent the spread of malaria is treatment of infected humans with drugs and indoor insecticide spraying. Otieno *et al.* [15] presented a SEIRS-SEI model for malaria transmission using four time-dependent control measures in Kenya. The authors concluded that the combination of treated bed nets and treatment of infected humans with anti-malarial drugs is the most efficient strategy to minimize the disease. Gashew *et al.* [16] presented an SIRS model for the human population and a climate-dependent SI model for malaria transmission that incorporates three controls. The authors suggest that the combination of the three controls (treated bed nets, treatment of infected humans with anti-malarial drugs and indoor insecticide spraying) is the best strategy to eliminate the disease. Similarly, notice

that optimal control modeling and cost-effectiveness analysis model have been applied in recent malaria models [17-23].

However, in these papers the influence of temperature variation on malaria epidemics using optimal control and cost-effectiveness analysis of using a logistic model for temperature variation with respect to mosquito breeding and contact rate was not considered. In this study, we considered a SIRS-SI model for malaria transmission with optimal control and analysis of cost-effectiveness in the presence of a logistic model for temperature variation with respect to the breeding rate and contact rate of mosquitoes.

This manuscript is organized as follows: in Section 2 we propose our model, which illustrates the impact of temperature variation on malaria epidemics. Section 3 provides the mathematical explanation of the model. Section 4 describes the sensitivity analysis of the parameters used in the model. In Section 5, the optimal control in malaria modeling is mathematically analyzed using Pontryagin's maximum principle. In Section 6, we present a simulation of the analytical results. In Section 7, the cost-effectiveness analysis is discussed. In Section 8 the conclusions of the work are given.

2 Model Description and Formulation

In this section, we formulate the SIRS-SI malaria transmission model, where the SIRS model represents the human population and the SI model the population represents the mosquito population. The total human population at time (t), denoted by $N_h(t)$, is divided into three sub-populations based on their disease status: susceptible humans, $S_h(t)$, that is: (1) those who are at risk of developing a malarial infection; (2) infected humans, $I_h(t)$, i.e. those who are showing symptoms of the disease and can transmit the disease to mosquitoes; and (3) recovered humans, $R_h(t)$, i.e. those who have temporary immunity and have recovered from the disease. Hence, the total human population is given by:

$$N_h(t) = S_h(t) + I_h(t) + R_h(t)$$

We assumed that all parameters in the system are positive. Individuals are born or migrate to the susceptible human population at rate Ψ. Susceptible humans become infected when they have contact with an infected mosquito at rate $\beta_h(T)$, which is dependent on temperature. β_{0h} is the human-to-mosquito contact rate when there is no temperature variation and β_{1h} is the increase of the contact rate due to temperature variation. Humans leave the total population at death rate μ_h and the malaria-induced death rate δ. Infected humans recover due to treatment using anti-malarial drugs at rate γ_h. The recovered population of humans whose immunity is not permanent can become susceptible to re-infection at rate ω_h. The

total vector population given by $N_m(t)$ at time (t) is sub-grouped into susceptible mosquitoes $S_m(t)$ and infected mosquitoes $I_m(t)$. Hence, the total vector population is given by $N_m(t) = S_m(t) + I_m(t)$. The vector population recruitment rate $\Phi(T)$ is dependent on temperature, while Φ_0 is the vector birth rate when there is no temperature variation and Φ_{1m} is the increasing vector birth rate due to temperature variation. A mosquito gets infected when it has contact with an infected human at rate $\beta_m(T)$, which is dependent on temperature, and β_{0m} is the vector-to-human contact rate when there is no temperature variation and β_{1m} is the increasing vector-to-human contact rate due to temperature variation. The vectors' natural death rate is μ_m. Mosquitoes do not die or recover from malaria infection. The temperature increase rate is denoted by r; T_{max} is the maximum temperature, when the vector is most active, whereas the minimum temperature, when the vector is least active, is denoted by T_0. Figure 1 shows a diagram of the transmission of malaria.

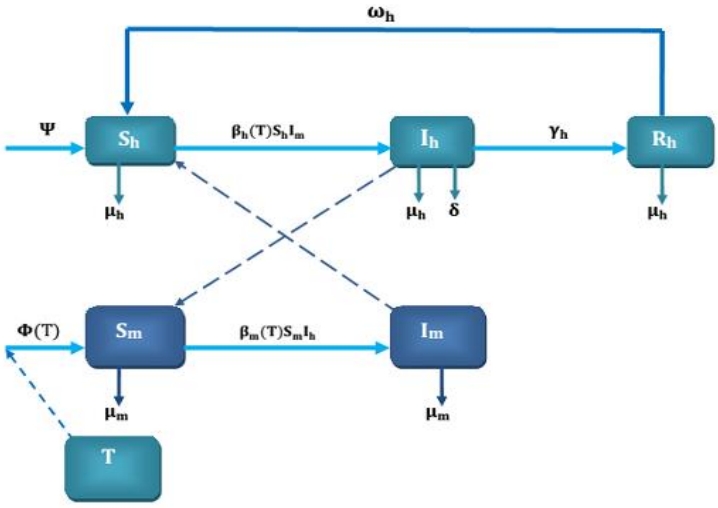

Figure 1 Malaria transmission diagram.

Using the flow chart described in Fig. 1, the model that governs the transmission of the disease is depicted by the following system of ordinary differential equations:

$$\begin{cases} \frac{dS_h}{dt} = \Psi - \beta_h(T)S_h I_m - \mu_h S_h + \omega_h S_h, \\ \frac{dI_h}{dt} = \beta_h(T)S_h I_m - (\mu_h + \delta + \gamma_h)I_h, \\ \frac{dR_h}{dt} = \gamma_h I_h - (\mu_h + \omega_h)R_h, \\ \frac{dS_m}{dt} = \Phi(T) - \beta_m(T)S_m I_h - \mu_m S_m, \\ \frac{dI_m}{dt} = \beta_m(T)S_m I_h - \mu_m I_m, \\ \frac{dT}{dt} = r\left(1 - \frac{T}{T_{max}}\right)(T - T_0) \end{cases} \quad (1)$$

where $\beta_h(T) = \beta_{0h} + \beta_{1h}\left(\frac{T-T_0}{T_{max}}\right)$, $\beta_m(T) = \beta_{0m} + \beta_{1m}\left(\frac{T-T_0}{T_{max}}\right)$, and $\Phi(T) = \Phi_0 + \Phi_{1m}\left(\frac{T-T_0}{T_{max}}\right)$.

with

$$\begin{aligned} &S_h(0) = S_{h0}, I_h(0) = I_{h0}, \\ &R_h(0) = R_{h0}, S_m(0) = S_{m0}, \\ &I_m(0) = I_{m0}, T(0) = T_{m0}\,. \end{aligned} \quad (2)$$

Table 1 Description of parameters used in Eq. 1.

Parameters	Parameter descriptions
Ψ	The rate at which new humans enter the population
Φ_0	Mosquito population recruitment rate
γ_h	Recovery rate of infected humans
μ_h	Natural death rate of the human population
δ	Induced death rate of the human population
μ_m	Natural death rate of the mosquito population
ω_h	Immunity loss rate of the human population
β_{0h}	Contact rate between humans and the mosquito population
Φ_{1m}	Increase of vector breeding rate
β_{0m}	Contact rate between mosquitoes and the human population
β_{1m}	Increase of vector contact rate
β_{1h}	Increase of human contact rate
r	Increase rate of the temperature
T_0	Minimum temperature when the vector is least active
T_{max}	Maximum temperature when the vector is most active

3 Mathematical Analysis of the Model

3.1 Invariant Region

To obtain the bounded region for model (1), first we consider the total human population given by $N_h(t) = S_h(t) + I_h(t) + R_h(t)$, differentiating both sides with respect to time. Then adding the first three equations from Eq. 1, we get

$$\frac{d}{dt}(S_h + I_h + R_h) = \Psi - \mu_h N_h - \delta I_h. \tag{3}$$

This implies that Eq. 3 becomes

$$\frac{d}{dt}(S_h + I_h + R_h) \leq \Psi - \mu_h N_h. \tag{4}$$

Integrating both sides of Eq. 4 and simplifying the expression, we obtain:

$$\Psi - \mu_h N_h \geq P e^{-\mu_h t}, \tag{5}$$

where P is a constant. Applying the initial conditions in Eq. 5 and rearranging the equation we get:

$$N_h \leq \frac{\Psi}{\mu_h} - \left(\frac{\Psi - \mu_h N_{h0}}{\mu_h}\right) e^{-\mu_h t}, \tag{6}$$

From Eq. 6, the size of the human population $N_h \to \frac{\Psi}{\mu_h}$ as $t \to \infty$, which shows that $0 < N_h \leq \frac{\Psi}{\mu_h}$. Thus, the invariant region of Eq. 1 for the human population is a positive invariant given by:

$$\Omega_h = \left\{(S_h, I_h, R_h) \in R_+^3 : 0 < S_h + I_h + R_h \leq \frac{\Psi}{\mu_h}\right\} \tag{7}$$

Secondly, the total number of the mosquito population from Eq. 1 is given as:

$$N_m(t) = S_m(t) + I_m(t). \tag{8}$$

Thus, the partial derivative of $N_m(t)$ with respect to time t is given by the following equation:

$$\frac{d}{dt}(S_m + I_m) = \Phi(T^*) - \mu_m N_m. \tag{9}$$

By solving Eq. 9, we obtain $0 < N_m \leq \frac{\Phi(T^*)}{\mu_m}$. Hence, the invariant region of Eq. 1 for the mosquito population, given by

$$\Omega_m = \left\{(S_m, I_m) \in R_+^2 : 0 < S_m + I_m \leq \frac{\Phi(T^*)}{\mu_m}\right\}, \tag{10}$$

is positively invariant. Consequently, the dynamics of Eq. 1 were studied in the invariant region of the form.

$$\Omega = \Omega_h \times \Omega_m = \left\{(S_h, I_h, R_h, S_m, I_m) \in R_+^5 : N_h \leq \frac{\Psi}{\mu_h}, N_m \leq \frac{\Phi(T^*)}{\mu_m}\right\} \quad (11)$$

is a positive invariant set under the flow induced by the solution set of Eq. 1.

3.2 Positivity of the Solution

For Eq. 1 we will show that all solutions of the system with positive initial data will remain positive for all times $t \geq 0$.

Theorem 1. If $S_h(0), I_h(0), R_h(0), S_m(0)$, and $I_m(0)$ are non-negative, then the solution $S_h(t),\ I_h(t), R_h(t), S_m(t)$, and $I_m(t)$ of Eq. 1 are non-negative for $t \geq 0$.

Proof. Take the first equation from Eq. 1 with $T^* \in \{T_0, T_{max}\}$:

$$\begin{aligned} \frac{dS_h}{dt} &= \Psi - \beta_h(T^*)S_h I_m - \mu_h N_h + \omega_h R_h \\ \frac{dS_h}{dt} &\geq -(\beta_h(T^*)I_m + \mu_h)S_h \end{aligned} \quad (12)$$

Integrating Eq. 12 with respect to time and using the method of variable separation while applying the initial conditions, we obtain:

$$S_h(t) \geq S_h(0)e^{-(\beta_h(T^*)I_m + \mu_h)t} \geq 0 \quad (13)$$

With the same procedure for other state variables, it can be shown that:

$$\begin{aligned} &I_h(t) \geq I_h(0)e^{-(\mu_h+\delta+\gamma_h)t} \geq 0, \\ &R_h(t) \geq R_h(0)e^{-(\mu_h+\omega_h)t} \geq 0, \\ &S_m(t) \geq S_m(0)e^{-(\beta_m(T^*)I_h+\mu_m)t} \geq 0, \\ &I_m(t) \geq I_m(0)e^{-\mu_m t} \geq 0. \end{aligned} \quad (14)$$

This shows that all solutions of Eq. 1 are non-negative for all $t \geq 0$. Therefore, the proposed malaria disease transmission model stated in Eq. 1 is both epidemiologically meaningful and mathematically well posed in feasible region Ω.

3.3 Disease Free Equilibrium (DFE)

The malaria free-equilibrium is the steady-state solution of Eq. 1 when there is no malaria disease. In order to get the disease-free equilibrium (DFE), we equate

all equations of Eq. 1 to zero with $I_h = 0, R_h = 0, I_m = 0$ and the obtained malaria-free equilibrium in Eq. 1 is denoted by E_1 or E_2, where:

$$E_1 = \left(\frac{\Psi}{\mu_h}, 0, 0, \frac{\Phi(T_0)}{\mu_m}, 0, T_0\right) \text{ or } E_2 = \left(\frac{\Psi}{\mu_h}, 0, 0, \frac{\Phi(T_{max})}{\mu_m}, 0, T_{max}\right) \tag{15}$$

3.4 Basic Reproduction Number

A basic reproductive number is described as the average amount of secondary infections caused by a primary infection in a given period [24]. It can be obtained using the next-generation matrix approach, i.e. the dominant eigenvalue of the next generation matrix. For Eq. 1, to obtain the R_{01} and R_{02} we rewrite Eq. 1 beginning with newly infective classes of humans and mosquito, given as:

$$\begin{aligned} \frac{dI_h}{dt} &= \beta_h(T^*)S_h I_m - (\mu_h + \delta + \gamma_h)I_h \\ \frac{dI_m}{dt} &= \beta_m(T^*)S_m I_h - \mu_m I_m \end{aligned} \tag{16}$$

Then, the right-hand side of Eq. 16 can be written in the form $f - v$, where

$$f = \begin{pmatrix} \beta_h(T^*)S_h I_m \\ \beta_m(T^*)S_m I_h \end{pmatrix} \text{ and } v = \begin{pmatrix} (\mu_h + \delta + \gamma_h)I_h \\ \mu_m I_m \end{pmatrix} \tag{17}$$

The partial derivatives of f and v at the disease-free equilibrium give the matrices F and V, respectively, where

$$F = \begin{pmatrix} 0 & \beta_h(T^*)\frac{\Psi}{\mu_h} \\ \beta_m(T^*)\frac{\Phi(T^*)}{\mu_m} & 0 \end{pmatrix} \text{ and } V = \begin{pmatrix} \mu_h + \delta + \gamma_h & 0 \\ 0 & \mu_m \end{pmatrix} \tag{18}$$

Hence, the basic reproduction number $R_0 = \rho(FV^{-1})$, where ρ is the largest eigenvalue of the product FV^{-1} and the R_0 at disease free-equilibrium points E_1 and E_2 are given by Eq. 19 and Eq. 20, respectively, as follows:

$$R_{01} = \sqrt{\frac{\beta_{0h}\Psi\beta_{0m}\Phi_0}{\mu_h\mu_m^2(\mu_h+\delta+\gamma_h)}} \tag{19}$$

and

$$R_{02} = \sqrt{\frac{(\beta_{0h}+\beta_{2h})\Psi(\beta_{0m}+\beta_{2m})(\Phi_0+\Phi_{2m})}{\mu_h\mu_m^2(\mu_h+\delta+\gamma_h)}} \tag{20}$$

where $\beta_{2h} = \beta_{1h}k, \beta_{2m} = \beta_{1m}k, \Phi_{2m} = \Phi_{1m}k$ and $k = \left(\frac{T_{max}-T_0}{T_{max}}\right)$.

Obviously, the basic reproduction number at maximum temperature (T_{max}) interim of R_{01} is obtained as:

$$R_{02} = \sqrt{R_{01}^2 + \frac{\Phi_0\beta_{0h}\beta_{2m} + \Psi(\beta_{0m}+\beta_{2m})[\beta_{2h}(\Phi_0+\Phi_{2m}) + \Phi_{2m}\beta_{0h}]}{\mu_h\mu_m^2(\mu_h+\delta+\gamma_h)}} \tag{21}$$

where R_{01} is the basic reproduction number at T_0, when the mosquitoes are least active in breeding.

3.5 Local Stability of Disease-Free Equilibrium

Theorem 2. The disease-free equilibrium point of Eq. 1 is locally asymptotically stable in Ω if $R_{01} < R_{02} < 1$.

Proof. We start by finding the Jacobian matrix of Eq. 1, given by:

$$J(E_*) = \begin{pmatrix} -\beta_h(T^*)I_h - \mu_h & 0 & \omega_h & 0 & -\beta_h(T^*)S_h \\ \beta_h(T^*)I_m & -(\mu_h+\delta+\gamma_h) & 0 & 0 & \beta_h(T^*)S_h \\ 0 & \gamma_h & J_{33} & 0 & 0 \\ 0 & -\beta_m(T^*)S_m & 0 & J_{44} & 0 \\ 0 & \beta_m(T^*)S_m & 0 & \beta_m(T^*)I_h & J_{55} \end{pmatrix} \tag{22}$$

where $J_{33} = -(\mu_h + \omega_h)$, $J_{44} = -\beta_m(T^*)I_h - \mu_m$, $J_{55} = -\mu_m$ and $T^* = T_0$ or T_{max}.

The result of the Jacobian matrix of Eq. 22 at the disease-free equilibrium is given by:

$$J(E_*) = \begin{pmatrix} -\mu_h & 0 & \omega_h & 0 & -\beta_h(T^*)\frac{\Psi}{\mu_h} \\ 0 & -(\mu_h+\delta+\gamma_h) & 0 & 0 & \beta_h(T^*)\frac{\Psi}{\mu_h} \\ 0 & \gamma_h & -(\mu_h+\omega_h) & 0 & 0 \\ 0 & -\beta_m(T^*)\frac{\Phi(T^*)}{\mu_m} & 0 & -\mu_m & 0 \\ 0 & \beta_m(T^*)\frac{\Phi(T^*)}{\mu_m} & 0 & 0 & -\mu_m \end{pmatrix}, \tag{23}$$

From Eq. 23, the Jacobian matrix is obtained as the polynomial function given by:

$$(-\lambda-\mu_h)(-\lambda-\mu_m)\big(-\lambda-(\mu_h+\omega_h)\big)(\lambda^2 + c_1\lambda + c_2) = 0 \tag{24}$$

where

$$c_1 = \mu_m + \mu_h + \delta + \gamma_h,$$
$$c_2 = \mu_m\gamma_h + \mu_m\delta + \mu_m\mu_h - \frac{\beta_h(T^*)\Psi\beta_m(T^*)\Phi(T^*)}{\mu_m\mu_h} \quad (25)$$

From Eq. 24 we get that

$$\lambda_1 = -\mu_h < 0, \lambda_2 = -\mu_m < 0, \lambda_3 = -(\mu_h + \omega_h) < 0 \quad (26)$$

and, again, from the last characteristic Eq. (24) we get,

$$\lambda^2 + c_1\lambda + c_2 = 0 \quad (27)$$

By using the Routh-Hurwitz criteria [25], Eq. 27 has a real root that is negative if $c_1 > 0$ and $c_2 > 0$. Hence, we can observe that $c_1 > 0$, since it is the sum of non-negative parameters and the value of c_2 at $T^* = T_{max}$ is given by:

$$C_2 = \mu_m\gamma_h + \mu_m\delta + \mu_m\mu_h - \frac{(\beta_{0h}+\beta_{2h})\Psi(\beta_{0m}+\beta_{2m})(\Phi_0+\Phi_{2m})}{\mu_m\mu_h}$$
$$= 1 - R_{02}^2 > 0$$

However, when c_2 is non-negative $1 - R_{02}^2$ could be positive, which implies that $R_{02} < 1$. Since $R_{01} < R_{02}$, the disease-free equilibrium is locally asymptotically stable if $R_{01} < R_{02} < 1$.

3.6 Global Stability of Disease Free-Equilibrium

Theorem 3. If $R_{01} < R_{02} < 1$, then the disease free-equilibrium point(s) of Eq. 1 are globally asymptotically stable in Ω.

Proof. To establish the stability, we use a technique implementing the Lyapunov theorem [26]. First, the Lyapunov function is developed, defined as:

$$V = \frac{\mu_m}{\beta_h(T^*)}I_h + I_m. \quad (28)$$

By differentiating the Lyapunov function with respect to time (t) the following result is obtained:

$$\frac{dV}{dt} = \frac{\mu_m}{\beta_h(T^*)}\frac{dI_h}{dt} + \frac{dI_m}{dt}$$
$$= \frac{\mu_m}{\beta_h(T^*)}(\beta_h(T)S_hI_m - (\mu_h + \delta + \gamma_h)I_h) + \beta_m(T)S_mI_h - \mu_mI_m$$
$$= \mu_mS_hI_m - \frac{\mu_m}{\beta_h(T^*)}(\mu_h + \delta + \gamma_h)I_h + \beta_m(T)S_mI_h - \mu_mI_m$$
$$= \left(\beta_m(T)S_m - \frac{\mu_m}{\beta_h(T^*)}(\mu_h + \delta + \gamma_h)\right)I_h - \mu_m(1 - S_h)I_m$$

$$\leq \left(\beta_m(T)S_m - \frac{\mu_m}{\beta_h(T^*)}(\mu_h + \delta + \gamma_h)\right) I_h$$

$$= \left(\beta_m(T)\frac{\Phi(T^*)}{\mu_m} - \frac{\mu_m}{\beta_h(T^*)}(\mu_h + \delta + \gamma_h)\right) I_h$$

$$= \frac{\mu_m(\mu_h+\delta+\gamma_h)}{(\beta_{0h}+\beta_{2h})}\left(\frac{\mu_h}{\Psi}R_{02}^2 - 1\right) I_h, \tag{29}$$

Consequently, we obtain $\frac{dV}{dt} < 0$ if $R_{02} < 1$ and $\frac{dV}{dt} = 0$ iff $I_h = 0, I_m = 0$. Thus, the dominant bounded invariant set in $\left\{(S_h, I_h, R_h, S_m, I_m) \in \Omega: \frac{dV}{dt} = 0\right\}$ is the singleton set DFE in Ω. Therefore, from LaSalle's invariant principle [27], every solution that begins in the domain approaches the DFE, as time tends to infinity and $R_{01} < R_{02}$; the DFE is globally asymptotically stable in Ω if $R_{01} < R_{02} < 1$.

3.7 Malaria Present Equilibrium

The malaria present equilibrium point is the situation where the malaria disease is found in the human population. The malaria present equilibrium point $E^* = (S_h^*, I_h^*, R_h^*, S_m^*, I_m^*, T^*)$ can be obtained by equating all the model equations in Eq. 1 to zero. Thus, from Eq. 1, the malaria present equilibrium point at $T^* = T_0$ is given by:

$$\begin{cases} S_h^* = \frac{\Psi+\omega_h R_h^*}{\beta_{0h}I_m^*+\mu_h}, \\ R_h^* = \frac{\gamma_h I_h^*}{\omega_h+\mu_h}, \\ S_m^* = \frac{\Phi_0}{\beta_{0m}I_h^*+\mu_m}, \\ I_m^* = \frac{\beta_{0m}S_h^*I_h^*}{\mu_m}. \end{cases} \tag{30}$$

From Eq. 30, the endemic equilibrium easily satisfies the following polynomial and I_h^* is computed with the following equation:

$$B_1(I_h^*)^2 + B_2(I_h^*) = 0, \tag{31}$$

where

$$\begin{aligned} B_1 &= \beta_{0m}\big(\beta_{0h}\Phi_0\big(\omega_h\delta + \mu_h(\gamma_h + \omega_h + \delta + \mu_h)\big) \\ &\qquad + \mu_h(\omega_h + \mu_h)(\gamma_h + \delta + \mu_h)\mu_m\big), \\ B_2 &= (\omega_h + \mu_h)[\mu_h\mu_m^2(\mu_h + \delta + \gamma_h)(1 - R_{01}^2)]. \end{aligned} \tag{32}$$

Hence, $B_1 > 0$ and $B_2 \geq 0$ whenever $R_{01} \geq 1$ solves I_h^*, we have that $I_h^* = -\frac{B_2}{B_1}$. Thus, the model has no non-negative malaria present equilibrium whenever $R_{01} < 1$. This illustrates that backward bifurcation does not exist in the model if $R_{01} < 1$.

Similarly, the endemic equilibrium points at $T^* = T_{max}$ and solving for I_h^* as parameter expressions we obtain:

$$\begin{cases} S_h^* = \frac{\Psi + \omega_h R_h^*}{(\beta_{0h} + \beta_{2h}) I_m^* + \mu_h}, \\ R_h^* = \frac{\gamma_h I_h^*}{\omega_h + \mu_h}, \\ S_m^* = \frac{(\Phi_0 + \Phi_{2m})}{(\beta_{0m} + \beta_{2m}) I_h^* + \mu_m}, \\ I_m^* = \frac{(\beta_{0m} + \beta_{2m}) S_h^* I_h^*}{\mu_m}, \end{cases} \tag{33}$$

where $\beta_{2h} = \beta_{1k},\ \beta_{2m} = \beta_{1k}, \Phi_{2m} = \Phi_{1k}$ and $k = \frac{T - T_0}{T_{max}}$.

From Eq. 33, the endemic equilibrium satisfies the following polynomial and I_h^* is computed with the following equation:

$$D_1 (I_h^*)^2 + D_2 (I_h^*) = 0, \tag{34}$$

where

$$\begin{aligned} D_1 = \beta_{3m} \big(& \beta_{3h} \Phi_{2m} \big(\omega_h \delta + \mu_h (\gamma_h + \omega_h + \delta + \mu_h) \big) \\ & + \mu_h (\omega_h + \mu_h)(\gamma_h + \delta + \mu_h) \mu_m \big) \\ D_2 = (\omega_h + \mu_h) & [\mu_h \mu_m^2 (\mu_h + \delta + \gamma_h)(1 - R_{02}^2)]. \end{aligned} \tag{35}$$

where $\beta_{3h} = \beta_{0h} + \beta_{2h},\ \beta_{3m} = \beta_{0m} + \beta_{2m}$ and $\Phi_{3m} = \Phi_0 + \Phi_{2m}$.

This implies that from Eq. 21, if $R_{02} < 1$ it is immediately implied that $R_{01} < 1$ and a DFE exists for both R_{01} and R_{02}. However, $R_{01} < 1$ does not immediately imply $R_{02} < 1$, as the value of R_{02} will be larger than unity, which shows that while R_{01} presents a DFE, R_{02} may create an endemic situation or show backward bifurcation, whereas R_{01} only presents forward bifurcation.

4 Sensitivity Analysis

Basically, by applying the normalized sensitivity index of the basic reproduction number to the given basic parameters we can express the robustness of the system's parameter value predictions, because the parameters can increase or

decrease the basic reproduction number if their values increase or decrease and vice versa. This approach requires us to identify the parameters that have the most influence on the basic reproduction number (R_{02}) in order to design the best control strategies for the disease. To conduct the sensitivity analysis, we followed the technique outlined in [13,28], which is defined as follows:

Definition 4.1: The forward sensitivity index of R_0, which is differentiable with respect to a given basic parameter D (see [13,28]), is defined as:

$$\tau_D^{R_0} = \frac{\partial R_0}{\partial D} \times \frac{D}{R_0}. \tag{36}$$

The sensitivity index of R_{01} in Eq. 1 with respect to parameter β_{0h}, for instance, is obtained as follows:

$$\begin{aligned} \tau_{\beta_{0h}}^{R_{01}} &= \frac{\partial R_{01}}{\partial \beta_{0h}} \times \frac{\beta_{0h}}{R_{01}} \\ &= \frac{1}{2\sqrt{\frac{\beta_{0h}\Psi\beta_{0m}\Phi_0}{\mu_h\mu_m^2(\mu_h+\delta+\gamma_h)}}} \times \frac{\Psi\beta_{0m}\Phi_0}{\mu_h\mu_m^2(\mu_h+\delta+\gamma_h)} \times \frac{\beta_{0h}}{R_{01}} \\ &= \frac{1}{2} > 0. \end{aligned} \tag{37}$$

Using the same approach with respect to the remaining parameters, $\tau_{\beta_{0m}}^{R_{01}}$, $\tau_{\Psi}^{R_{01}}$, $\tau_{\Phi_0}^{R_{01}}$, $\tau_{\mu_h}^{R_{01}}$, $\tau_{\mu_m}^{R_{01}}$, $\tau_{\delta}^{R_{01}}$, $\tau_{\gamma_h}^{R_{01}}$ are computed and the sensitivity indices are obtained as described in Table 2.

Table 2 Parameter of sensitivity indices.

Parameter	Sensitivity index
Ψ	0.5
Φ_0	0.5
β_{0h}	0.5
β_{0m}	0.5
μ_m	1
μ_h	-0.092541
δ	-0.475258
γ_h	-0.024461

By the same procedure, the sensitivity index of R_{02} from Eq. 1 with respect to Ψ is given as:

$$\Pi_{\Psi}^{R_{02}} = \frac{\partial R_{02}}{\partial \Psi} \times \frac{\Psi}{R_{02}} \tag{38}$$

$$= \frac{1}{2\sqrt{\frac{(\beta_{0h}+\beta_{2h})\Psi(\beta_{0m}+\beta_{2m})(\Phi_0+\Phi_{2m})}{\mu_h\mu_m^2(\mu_h+\delta+\gamma_h)}}} \times \frac{(\beta_{0h}+\beta_{2h})(\beta_{0m}+\beta_{2m})(\Phi_0+\Phi_{2m})}{\mu_h\mu_m^2(\mu_h+\delta+\gamma_h)} \times \frac{\Psi}{R_{02}}$$

$$= \frac{1}{2} > 0$$

Similarly, with respect to the other basic parameters, $\Pi_{\beta_{0h}}^{R_{02}}$, $\Pi_{\beta_{0m}}^{R_{02}}$, $\Pi_{\Psi}^{R_{02}}$, $\Pi_{\Phi_0}^{R_{02}}$, $\Pi_{\beta_{1m}}^{R_{02}}$, $\Pi_{\Phi_{1m}}^{R_{02}}$, $\Pi_{\mu_h}^{R_{02}}$, $\Pi_{\mu_m}^{R_{02}}$, $\Pi_{\delta}^{R_{02}}$, $\Pi_{\gamma_h}^{R_{02}}$ are computed and the sensitivity indices are described in Table 3.

Table 3 Parameter of sensitivity indices.

Parameter	Sensitivity index
Ψ	0.5
Φ_0	0.072438
β_{0h}	0.291659
β_{0m}	0.285714
Φ_{1m}	0.069169
β_{1h}	0.208341
β_{1m}	0.214286
μ_m	-1
μ_h	-0.092541
δ	-0.475258
γ_h	-0.024461

4.1 Interpretation of the Sensitivity Indices

In Table 2 we give the sensitivity indices of R_{01} with respect to the basic parameters. This result shows that the parameters $\Psi, \Phi_0, \beta_{0h},$ and β_{0m} have positive sensitivity indeces and the value of R_{01} increase when their values are increased while the other parameters stay constant. The parameters μ_m, μ_h, δ and γ_h have negative indices and the value of R_{01} increase if their values are increased while the other parameters stay constant. Similarly, in Table 3, the sensitivity indices of R_{02} with respect to the basic parameters are shown. The basic parameters having a positive sensitivity index could have an impact on the transmission of malaria in the population as their value increases. The basic parameters whose sensitivity indices are negative increase the malaria disease if their values decrease while the other parameters stay constant. For instance, $\Pi_{\Psi}^{R_{02}} = 0.5$, shows that decreasing (increasing) the rate of human recruitment by 10% decreases (increases) the basic reproduction number R_{02} by 5%. Similarly, $\Pi_{\mu_m}^{R_{02}} = -1$ indicates that decreasing (increasing) the mosquito death rate by 10% increases (decreases) the basic reproduction number R_{02} by 10%.

Table 4 Parameter descriptions and values used for Eq. 1.

Parameters	Parameters' description	Values	References
γ_h	Infected human recovery rate	0.0035	[25]
Ψ	Human population recruitment rate	0.071	[29]
Φ_0	Mosquito population recruitment rate	0.041	[28]
μ_m	Mosquito population natural death rate	0.05	[25]
μ_h	Human population natural death rate	0.00004	[13]
δ	Human population induced death rate	0.068	[30]
ω_h	Immunity loss rate of human population	0.09	[31]
β_{1m}	Increase of vector breeding rate	0.07	[31]
β_{1h}	Increase of human contact rate	0.05	[31]
Φ_{1m}	Increase of vector contact rate	0.09	[31]
β_{0h}	Human-to-mosquito contact rate	0.03	[32]
β_{0m}	Mosquito-to-humans contact rate	0.04	[13]
r	Temperature growth rate	0.007	[31]
T_0	Minimum temperature	16 ℃	[11]
T_{max}	Maximum temperature	28 ℃	[33]

5 Extension of The Model into Optimal Control

In this study, we extended the basic malaria model in Eq. 1 to an optimal control problem involving a mathematical model of the biological situation [34]. Using this approach, we want to find the optimal strategy for prevention of the disease. After incorporating the controls into the basic malaria model in Eq. 1, the state equations obtained is:

$$\begin{cases} \frac{dS_h}{dt} = \Psi - (1-u_1)\beta_h(T)S_hI_m - \mu_h S_h + \omega_h R_h\,, \\ \frac{dI_h}{dt} = (1-u_1)\beta_h(T)S_hI_m - (\mu_h + \delta + \gamma_h + u_2)I_h, \\ \frac{dR}{dt} = (\gamma_h + u_2)I_h - (\mu_h + \omega_h)R_h, \\ \frac{dS_m}{dt} = \phi(T) - (1-u_1)\beta_m(T)S_mI_h - (\mu_m + u_3)S_m, \\ \frac{dI_m}{dt} = (1-u_1)\beta_m(T)S_mI_h - (\mu_m + u_3)I_m, \\ \frac{dT}{dt} = r\left(1 - \frac{T}{T_{max}}\right)(T - T_0), \end{cases} \tag{39}$$

where, $\beta_h(T) = \beta_{0h} + \beta_{1h}(\frac{T-T_0}{T_{max}})$, $\beta_m(T) = \beta_{0m} + \beta_{1m}(\frac{T-T_0}{T_{max}})$ and $\phi(T) = \phi_0 + \phi_{1m}(\frac{T-T_0}{T_{max}})$.

The control functions denote that $u_1(t)$ is the use of treated bed nets; $u_2(t)$ denotes treatment of infected humans with anti-malarial drugs; and $u_3(t)$ denotes

indoor residual insecticide spraying to kill mosquitoes. The objective functional we formulated for Eq. 39 is given by:

$$J(u_1, u_2, u_3) = min \int_0^{t_f} [A_1 I_h + A_2 I_m + \tfrac{1}{2}(B_1 u_1^2 + B_2 u_2^2 + B_3 u_3^2)]dt \quad (40)$$

where t_f denotes the final time, A_1 and A_2 are constants given for infectious humans and infectious mosquitoes respectively, while B_1, B_2 and B_3 are weight constants for each control, respectively. The expression $\frac{1}{2}B_i u_i^2$ stands for the cost function that corresponds to the controls $u_i(t)$, which is quadratic in accordance with the literature [22,23,35,36]. The aim of the objective function Eq. 40 is to reduce the total amount of infectious humans $I_h(t)$, infectious mosquitoes $I_m(t)$, and the costs associated with controls $u_i(t)$. The main goal is to compute a triple optimal control u_1^*, u_2^* and u_3^* such that

$$J(u_1^*, u_2^*, u_3^*) = min\{J(u_1, u_2, u_3): u_1, u_2, u_3 \in \vartheta\} \quad (41)$$

where $\vartheta = (u_1, u_2, u_3): u_i(t)$ such that u_1, u_2 and u_3 are Lebesgue measurable on $t \in [0, t_f]$ with $0\, w u_i(t) \leq 1$ as the control set. To obtain the necessary conditions for optimal control model Eq. 39, we apply Pontryagin's maximum principle [37]. The defined Hamiltonian (H) function of the optimal control problem that consists of Eq. 39 and Eq. 40 is represented as

$$\begin{aligned} H = {} & \left[A_1 I_h + A_2 I_m + \tfrac{1}{2}\sum_{i=1}^{3} B_i\, u_i^2\right] + \lambda_1 \tfrac{dS_h}{dt} + \lambda_2 \tfrac{dI_h}{dt} \\ & + \lambda_3 \tfrac{dR_h}{dt} + \lambda_4 \tfrac{dS_m}{dt} + \lambda_5 \tfrac{dI_m}{dt} + \lambda_6 \tfrac{dT}{dt}. \end{aligned} \quad (42)$$

It follows that the system of Eq. 39 and Eq. 40 are substituted into a minimized Hamiltonian function with respect to u_1, u_2, u_3 as given by:

$$\begin{aligned} H = {} & \left[A_1 I_h + A_2 I_m + \tfrac{1}{2} B_1 u_1^2 + B_2 u_2^2 + B_3 u_3^2\right] \\ & + \lambda_1 \left(\Psi - (1-u_1)\beta_h(T) S_h I_m - \mu_h S_h + \omega_h R_h\right) \\ & + \lambda_2 \left((1-u_1)\beta_h(T) S_h I_m - (\mu_h + \delta + \gamma_h + u_2) I_h\right) \\ & + \lambda_3 \left((\gamma_h + u_2) I_h - (\mu_h + \omega_h) R_h\right) \\ & + \lambda_4 \left(\phi(T) - (1-u_1)\beta_m(T) S_m I_h - (\mu_m + u_3) S_m\right) \\ & + \lambda_5 \left((1-u_1)\beta_m(T) S_m I_h - (\mu_m + u_3) I_m\right) \\ & + \lambda_6\, r\left(1 - \tfrac{T}{T_{max}}\right)(T - T_0), \end{aligned} \quad (43)$$

where λ_1, λ_2, λ_3, λ_4, λ_5 and λ_6 are adjoint variables. Next to obtaining the co-state variables by using Pontryagin's maximum principle [37], with the existence result from [38], the following theorem is stated:

Theorem 6. For given optimal control triples u_1^*, u_2^*, u_3^* and a solution $S_h^*, I_h^*, R_h^*, S_m^*, I_m^*, T^*$ of the corresponding state system that minimizes $J(u_1, u_2, u_3)$ over ϑ subject to Eq 39, adjoint variables λ_1, λ_2, λ_3, λ_4, λ_5 and λ_6 are found, holding the adjoint system

$$\begin{cases} \frac{d\lambda_1}{dt} = -\big((1-u_1)\beta_h(T)I_m(\lambda_2-\lambda_1)\big) + \mu_h\lambda_1, \\ \frac{d\lambda_2}{dt} = -\big((1-u_1)\beta_h(T)S_m(\lambda_5-\lambda_4)\big) + \lambda_2(\mu_h + \delta + \gamma_h + u_2) \\ \qquad -\lambda_3(\gamma_h + u_2) - A_1, \\ \frac{d\lambda_3}{dt} = -\omega_h\lambda_1 + \lambda_3(\mu_h + \omega_h), \\ \frac{d\lambda_4}{dt} = -\big((1-u_1)\beta_m(T)I_h(\lambda_5-\lambda_4)\big) + \lambda_4(\mu_m + u_3), \\ \frac{d\lambda_5}{dt} = -\big((1-u_1)\beta_m(T)S_h(\lambda_2-\lambda_1)\big) + \lambda_4(\mu_m + u_3) - A_2, \\ \frac{d\lambda_6}{dt} = r\,\lambda_6 - r\,\lambda_6\left(\frac{T_0}{T_{max}} - \frac{T}{T_{max}}\right), \end{cases} \tag{44}$$

with transversality conditions

$$\lambda_1(t_f) = \lambda_2(t_f) = \lambda_3(t_f) = \lambda_4(t_f) = \lambda_5(t_f) = \lambda_6(t_f) = 0 \tag{45}$$

Furthermore, the optimal controls u_1^*, u_2^*, u_3^* are represented by:

$$\begin{aligned} u_1^* &= max\left\{0, min\left\{1, \frac{(\lambda_2-\lambda_1)\beta_h(T)S_h^*I_m^* + (\lambda_5-\lambda_4)\beta_m(T)S_m^*I_h^*}{B_1}\right\}\right\}, \\ u_2^* &= max\left\{0, min\left\{1, \frac{(\lambda_2-\lambda_3)I_h^*}{B_2}\right\}\right\}, \\ u_3^* &= max\left\{0, min\left\{1, \frac{\lambda_4 S_m^* + \lambda_5 I_m^*}{B_3}\right\}\right\}. \end{aligned} \tag{46}$$

Proof. To obtain the form of the co-state equations we compute the derivative of the Hamiltonian function (H), Eq. 42, with respect to S_h, I_h, R_h, S_m, I_m and T respectively. Then the adjoint or co-state equations obtained are given by:

$$\begin{cases} \frac{d\lambda_1}{dt} = \frac{\partial H}{\partial S_h} = -\big((1-u_1)\beta_h(T)I_m(\lambda_2-\lambda_1)\big) + \mu_h\lambda_1, \\ \frac{d\lambda_2}{dt} = \frac{\partial H}{\partial I_h} = -\big((1-u_1)\beta_h(T)S_m(\lambda_5-\lambda_4)\big) \\ \qquad +\lambda_2(\mu_h + \delta + \gamma_h + u_2) - \lambda_3(\gamma_h + u_2) - A_1, \\ \frac{d\lambda_3}{dt} = \frac{\partial H}{\partial R_h} = -\omega_h\lambda_1 + \lambda_3(\mu_h + \omega_h), \\ \frac{d\lambda_4}{dt} = \frac{\partial H}{\partial S_m} = -\big((1-u_1)\beta_m(T)I_h(\lambda_5-\lambda_4)\big) + \lambda_4(\mu_m + u_3), \\ \frac{d\lambda_5}{dt} = \frac{\partial H}{\partial I_m} = -\big((1-u_1)\beta_m(T)S_h(\lambda_2-\lambda_1)\big) \\ \qquad +\lambda_4(\mu_m + u_3) - A_2, \\ \frac{d\lambda_6}{dt} = \frac{\partial H}{\partial T} = r\,\lambda_6 - r\,\lambda_6\left(\frac{T_0}{T_{max}} - \frac{T}{T_{max}}\right), \end{cases} \tag{47}$$

with transversality conditions

$$\lambda_1(t_f) = \lambda_2(t_f) = \lambda_3(t_f) = \lambda_4(t_f) = \lambda_5(t_f) = \lambda_6(t_f) = 0 \tag{48}$$

To obtain the control values, we compute the partial derivative of the Hamiltonian, given by:

$$\frac{\partial H}{\partial u_i} = 0 \text{ for } i = 1,2,3. \tag{49}$$

Obviously, after derivation of function (H), Eq. 42, with respect to the controls, the result becomes:

$$\begin{aligned} 0 &= \frac{\partial H}{\partial u_1} = (\lambda_1 - \lambda_2)\beta_h(T)S_h^* I_m^* + (\lambda_4 - \lambda_5)\beta_m(T)S_m^* I_h^* + u_1 B_1, \\ 0 &= \frac{\partial H}{\partial u_2} = \lambda_3 I_h^* - \lambda_2 I_h^* + u_2 B_2, \\ 0 &= \frac{\partial H}{\partial u_3} = -(\lambda_4 S_m^* + \lambda_5 I_m^*) + u_3 B_3. \end{aligned} \tag{50}$$

Moreover, solving for the control variables from Eq. 50 we obtain:

$$\begin{aligned} u_1^* &= \frac{(\lambda_2-\lambda_1)\beta_h(T)S_h^* I_m^* + (\lambda_5-\lambda_4)\beta_m(T)S_m^* I_h^*}{B_1}, \\ u_2^* &= \frac{(\lambda_2-\lambda_3)I_h^*}{B_2} \\ u_3^* &= \frac{\lambda_4 S_m^* + \lambda_5 I_m^*}{B_3}. \end{aligned} \tag{51}$$

Rearranging the solution of Eq. 51 with the boundary condition of each control, we get:

$$\begin{aligned} u_1^* &= max\left\{0, min\left\{1, \frac{(\lambda_2-\lambda_1)\beta_h(T)S_h^* I_m^* + (\lambda_5-\lambda_4)\beta_m(T)S_m^* I_h^*}{B_1}\right\}\right\}, \\ u_2^* &= max\left\{0, min\left\{1, \frac{(\lambda_2-\lambda_3)I_h^*}{B_2}\right\}\right\} \\ u_3^* &= max\left\{0, min\left\{1, \frac{\lambda_4 S_m^* + \lambda_5 I_m^*}{B_3}\right\}\right\}. \end{aligned} \tag{52}$$

Next, we investigated a simulation of the optimal control problem to identify the optimal strategy, which is the most effective in preventing malaria disease transmission.

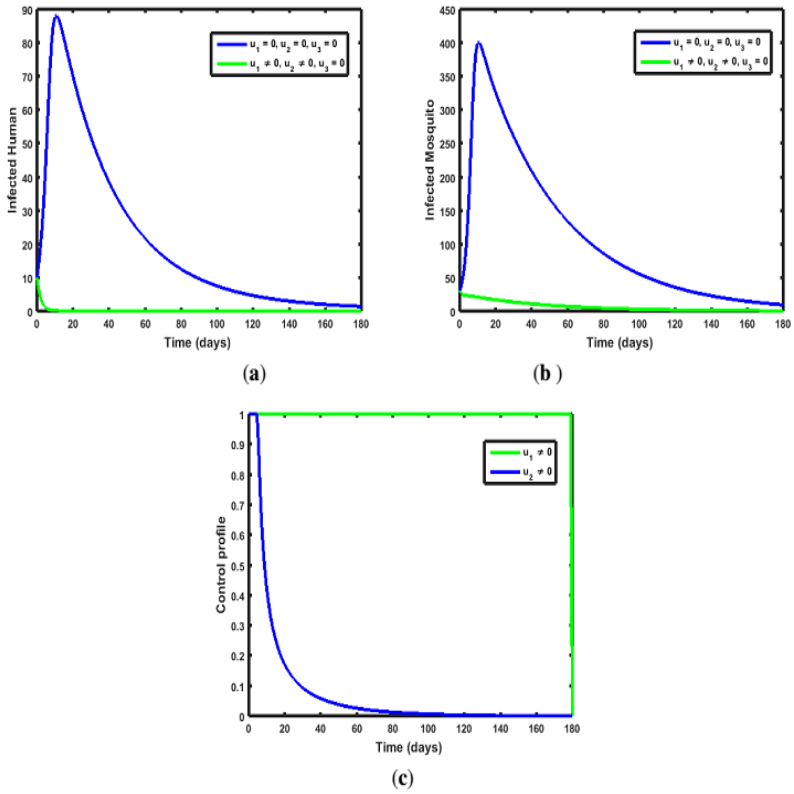

Figure 2 Simulations showing the use of treated bed nets (u_1) and treatment of and treatment of infectious with drugs (u_2).

6 Numerical Simulation

In this study, to get the optimal strategy we solved an optimality system that contained two systems, i.e. six ordinary differential systems from the state equations and six from the adjoint equations. To solve the state system and the adjoint system, the forward-backward sweep method was used. In solving state equations Eq. 39, due to the initial value of the state variables, the forward fourth order Runge-Kutta was used. We solved the adjoint equations using the backward fourth order Runge Kutta due to the transversality condition in Eq. 45, holding the state equations solution and optimal controls values. Then the controls were updated, applying a convex combination of the controls existing before and the optimality condition values of Eq. 46. This situation can continue until two consecutive iterations are very close to each other [34]. For numerical simulation of the optimality system, the initial condition that we used was: $S_h(0) = 100$, $I_h(0) = 10$, $R_h(0) = 0$, $S_m(0) = 300$, $I_m(0) = 30$, T(0) = 16 °C and the

parameter values from Table 4 were used, where $R_{01} = 33.14$ and $R_{02} = 78.87$ are basic reproduction numbers. The weight constant values chosen for the state and controls that we used were: $A_1 = 60$, $A_2 = 80, B_1 = 40$, $B_2 = 100$ and $B_3 = 60$. Also, we propose the following four strategies with different combinations of more than one control at the same time to show the impact of the controls on reducing disease transmission.

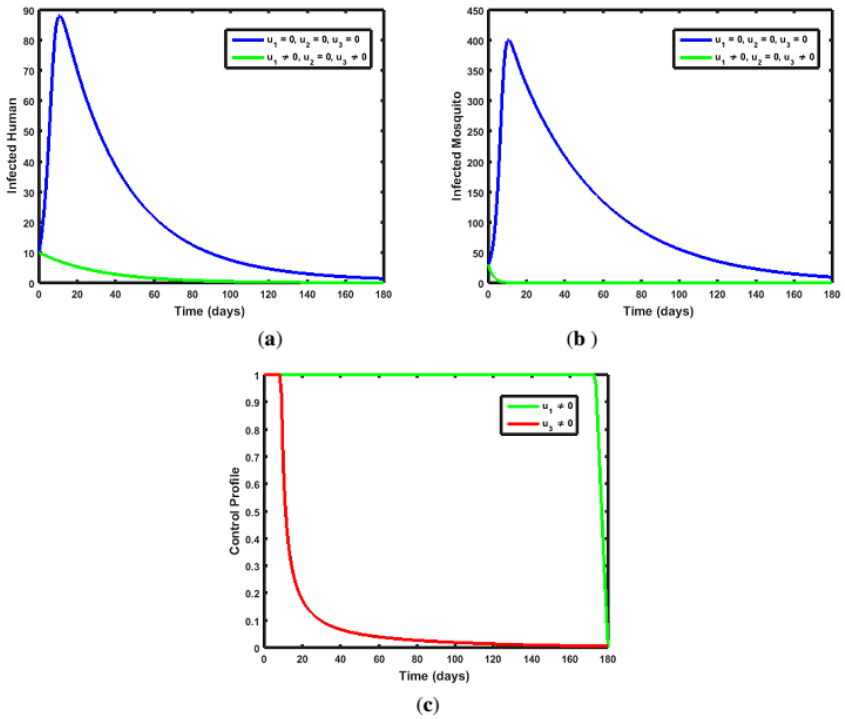

Figure 3 Simulations showing the use of infected humans (u_1) and indoor insecticide spraying (u_3) as controls.

6.1 Strategy A: Combination of Use of Treated Bed Nets (u_1) and Treatment of Infected (u_2)

Under this strategy, the objective function Eq. 40 is optimized, with treated bed nets as control u_1 and the treatment of infected humans as control u_2 and the value of indoor insecticide spraying as control u_3 set to zero. From Fig. 2(a) we can see that when the number of infected humans I_h decreased, it tended towards its lowest point, whereas the number of infected humans increased when no control was used. Similarly, in Fig. 2(b) we can see that the number of infected mosquitoes I_m decreased when the control strategy was used and tended towards its lowest point, whereas when no control was used, the number of infected

mosquitoes increased. The control profiles with this strategy, as shown in Fig. 2(c), suggest that the control of using treated bed nets u_1 maintained its maximum level (100%) until the end of the implementation while the control of the treatment of infected humans u_2 retained its highest bound for 5 days and then declined until it reached its minimum value after the 80th day.

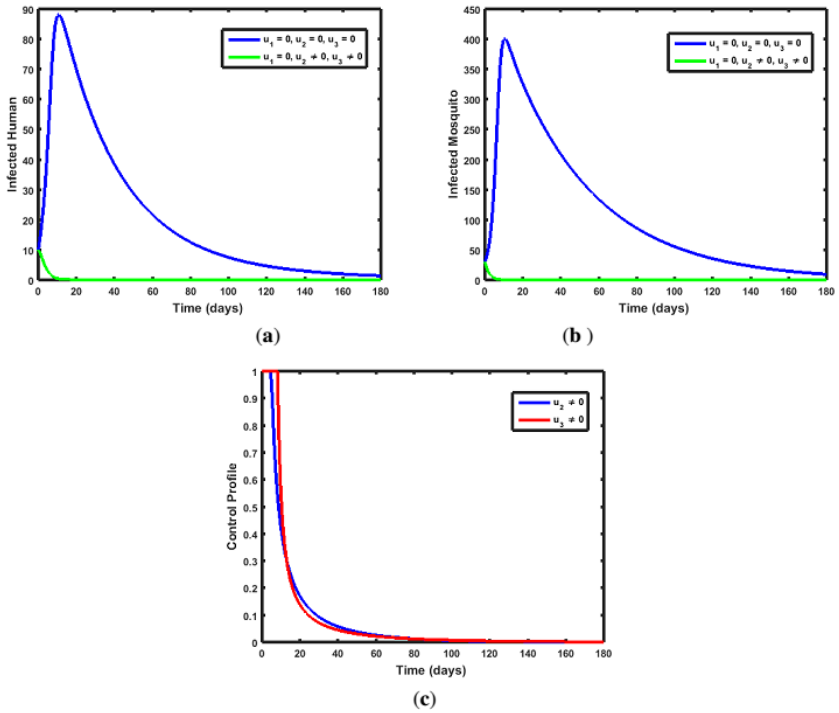

Figure 4 Numerical simulations showing treatment of infected humans (u_2) and indoor insecticide spraying (u_3) as controls.

6.2 Strategy B: Combination of the Use of Treated Bed Nets (u_1) and Insecticide Spraying (u_3)

This strategy combines the control of treated bed nets u_2 and the control of indoor insecticide spraying u_3 to reduce the total infected population and the associated costs, without treatment of infected humans u_2. In Fig. 3(a) we can see that the number of infected humans I_h decreased to its lowest point. In contrast, the number of infected humans increased up to a certain point when no controls were used. From Fig. 3(b) we can see that the number of infected mosquitoes I_m decreased when there was a control strategy and decreased to its minimum point, while the number of infected mosquitoes increased for the case without control. The control profiles in Fig. 3(c) suggest that the control of treated

bed nets u_1 maintained its maximum value (100%) for 170 days, whereas the control of insecticide spraying u_3 retained its highest bound for 8 days, after which it reached its lowest value after the 120th day.

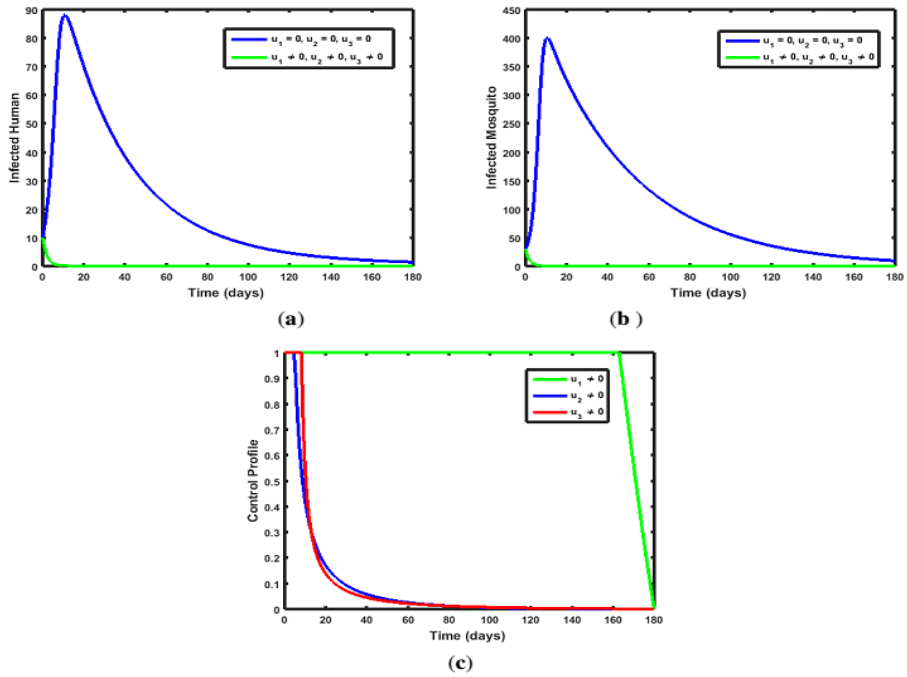

Figure 5 Simulations result with treated bed nets (u_1), treatment of infected humans (u_2) and insecticide spraying (u_3) as controls.

6.3 Strategy C: Combination of Treatment of Infected Humans (u_2) and Insecticide Spraying (u_3)

In this strategy, to minimize Eq. 40 we use a combination of the control of treatment of infected humans u_2 and the control of indoor insecticide spraying u_3 to minimize the total infected population and reduce the costs. From Fig. 4(a) we can see that with this control strategy, the number of infected humans I_h became smaller with the use of this control strategy than without the use of controls and declined to its lowest value. The number of infected mosquitoes I_m decreased with the use of this control strategy and then dropped to its minimum value, whereas in the case without control and the number infected mosquitoes increased, as can be seen in Fig. 4(b). In Fig. 4(c), with this approach the control profiles show that the treatment of infected humans u_2 maintained its highest value (100%) for 8 days, while insecticide spraying u_3 maintained its maximum value for 6 days, then decreased and reached its lower bound after the 80th day.

6.4 Strategy D: Use of Treated Bed Net (u_1), Treatment (u_2) and Spray of Insecticides (u_3).

To minimize Eq. 40, we applied three controls: treated bed nets u_1, treatment of infected humans u_2, and indoor insecticide spraying u_3. From Fig. 5(a) we can see that with applying these three controls, the number of infected humans I_h decreased to the minimum level while the number of infected humans increased to a certain point when there was no use of any controls. It can be said that the population of infected mosquitoes I_m decreased because of the use of this control strategy and decreased to its lowest bound, whereas in the absence of a control strategy the number of infected mosquitoes increased, as shown in Fig. 5(b). Using this strategy, Fig. 5(c) shows that treatment of infected humans u_2 and indoor insecticide spraying u_3 kept their maximum value (100%) for 8 days and 5 days, respectively. Then they declined and reached their lowest bound after 80 days, while treated bed nets u_1 retained its highest value (100%) for 162 days and then started decreasing and reached its minimum level on the 100th day.

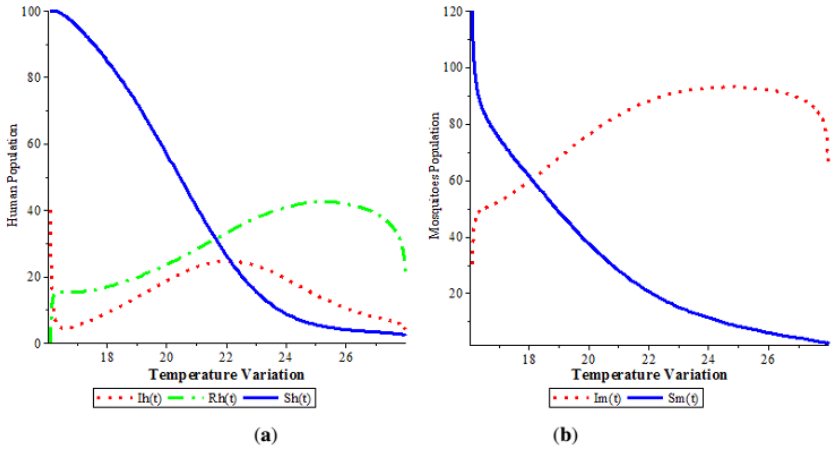

Figure 6 Human population and mosquito population with temperature variation.

Fig. 6 describes the human population and the mosquito population against temperature variation. From Fig. 6(a) we can see that the susceptible human population decreased and then reached zero at the maximum temperature ($T_{max} = 28$°C); the recovered human population increased to a certain maximum point and then decreased, and the population of infected humans decreased to a certain point and then decreased at the maximum temperature ($T_{max} = 28$°C). It can also be seen in Fig. 6(b) that the infected mosquito population increased to a maximum point and then decreased, while the susceptible mosquito population decreased and reached zero at the maximum temperature ($T_{max} = 28$°C).

Fig. 7 shows the bifurcation diagram in which T = T_0 and T = T_{max} for the malaria model problem. The model exhibited forward and backward bifurcation, respectively. Moreover, the biological concept of this implies that from Eq. 21, $R_{02} < 1$ immediately implies that $R_{01} < 1$ and a DFE exists for both R_{01} and R_{02}. However, $R_{01} < 1$ does not immediately imply $R_{02} < 1$, as the value of R_{02} will be larger than unity, whereas R_{01} exhibits a DFE, R_{02} may create an endemic situation or show backward bifurcation, whereas R_{01} only exhibits forward bifurcation.

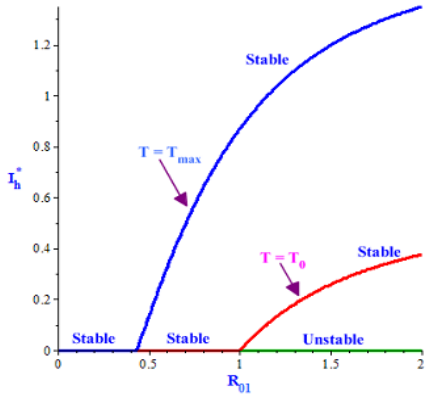

Figure 7 Bifurcation diagram shows T = T_0 and T = T_{max} for the malaria model problem.

7 Cost Effectiveness Analysis

Based on the simulation result of the optimality system using the parameter values in Table 4, we can find the most effective and least costly strategy. To obtain this strategy, we applied the approach called incremental cost-effectiveness ratio (ICER). Applying this technique we compared more-than-unity competing strategies to compare an intervention with the next less effective alternative. This approach was defined as the ratio of the difference in averted costs between two strategies to the difference in the total number of infections saved [39]. From the simulation result of the optimal control problem, we calculated the total cost averted, the total number of infections saved. In Table 5, the control strategies are ordered in increasing order based on the total number of infections saved. The total number of infections saved was computed as the difference between the total number of the human population with malaria infection with controls and the total number of the human population with malaria infection without controls, whereas the cost averted of each strategy was obtained by using the cost function represented by $\frac{1}{2}B_1u_1^2$, $\frac{1}{2}B_2u_2^2$ and $\frac{1}{2}B_3u_3^2$ over time

[39]. The total number of infections saved and the total cost of all strategies with their ICER is given in Table 6. However, we did not consider a strategy that applies only one single control, since a single control is not effective in removing the malaria disease completely from the human population.

Table 5 Total number of infections saved and cost averted for all strategies.

Strategy	Description	Total Infections Averted	Total Cost ($)
A	Treated bed nets and insecticide spraying	3792.797	6420.361
C	Treatment of infected humans and insecticide spraying	4094.558	1955.467
B	Treated bed nets and treatment of infected humans	4115.460	6474.615
D	Treated bed nets, treatment of infected humans and insecticide spraying	4115.486	6490.286

Having the total number of infections saved and cost averted for each strategy in Table 5, the value of incremental cost-effectiveness ratio (ICER) was computed to compare the difference between two strategies, as obtained by:

$$\text{ICER (B)} = \frac{6420.361}{3792.797} = 1.693$$

$$\text{ICER (C)} = \frac{1955.467 - 6420.361}{4094.558 - 3792.797} = -14.796$$

$$\text{ICER (A)} = \frac{6474.615 - 1955.467}{4115.460 - 4094.5584} = 216.211$$

$$\text{ICER (D)} = \frac{6490.286 - 6474.615}{4115.486 - 4115.460} = 602.725$$

From the above result, the number of infections saved with ICER for the four different strategies is given in Table 6.

Table 6 Total number of infections saved and cost averted used with ICER.

Strategy	Number of Infections Saved	Total Cost ($)	ICER
B	3792.797	6420.361	1.693
C	4094.558	1955.467	-14.796
A	4115.460	6474.615	216.211
D	4115.486	6490.286	602.725

In Table 6 we compare interventions B and C. It can be seen that ICER (C) was smaller than ICER (B). This shows that strategy B is more expensive and less effective at saving people. Thus, Strategy C saves more people than strategy B. Strategy B was omitted as a competing strategy. Then, we computed the ICER for the other strategies, C, A and D, as shown in Table 7.

As can be seen in Table 7 ICER (A) was larger than ICER (C). This shows that intervention C outperforms A. That is, strategy A is less effective and more costly than strategy C. Hence, we dropped strategy A from the group of competitors and re-computed ICER as shown in Table 8.

Table 7 Total number of infections saved and cost averted used with ICER.

Strategy	Number of Infections Saved	Total Cost ($)	ICER
C	4094.558	1955.467	0.478
A	4115.460	6474.615	216.211
D	4115.486	6490.286	602.725

In Table 8, the comparison between intervention strategies C and D indicates that ICER (D) was higher than ICER (C). This immediately shows that strategy C highly outperforms D. Strategy C yielded the lowest total cost and the highest effectivity. Based on the result of the analysis, we therefore recommend intervention C, which is a combination of treatment of infected humans and insecticide spraying, as the most effective and least costly strategy to minimize the spread of the malaria disease.

Table 8 Total number of infections saved and cost averted with ICER.

Strategy	Number of Infections Saved	Total Cost ($)	ICER
C	4094.558	1955.467	0.478
D	4115.486	6490.286	216.687

8 Conclusion

In this paper, deterministic mathematical modeling of the influence of temperature variability on malaria epidemics is described. Qualitatively, the model analysis showed that the model is both bounded and positive within a fixed domain. The reproductive number along the malaria-free equilibrium was estimated using the next-generation matrix technique. Applying the Jacobian matrix and Lyapunov method, the local and global stability of the malaria-free equilibrium were shown respectively. Thus, if the reproductive number is smaller than one, then the malaria-free equilibrium is both locally and globally asymptotically stable, whereas a positive endemic equilibrium occurs if the reproductive number is greater than unity. The analysis of the sensitivity of the model was described; the model exhibited forward and backward bifurcation. Temperature variation has an impact on the transmission of malaria. The human-to-mosquito contact rate, the mosquito-to-human contact rate, and the mosquito breeding rate increased. It was observed that increasing these parameters led to an increase in the basic reproductive number, which makes it harder to control

the disease. From the analytical results of this study, we conclude that the most efficient way to control a malaria epidemic is to decrease the human-to-mosquito contact rate, increase the death rate of mosquitoes, and increase the treatment rate of infected humans with anti-malarial drugs. Moreover, we extended the model to an optimal control problem using three controls: using treated bed nets, treatment of infected humans using anti-malarial drugs, and indoor residual insecticide spraying. Pontraygin's maximum principle was applied to compute the conditions for the optimal control strategy and a cost-effectiveness analysis was conducted using all the various combinations of the three controls considered in this study. From the result of a simulation with the optimality system and analysis of cost-effectiveness, we conclude that the combination of treatment of infected humans and insecticide spraying is the optimal strategy to effectively eradicate malaria.

Acknowledgements

This work was supported by Adama Science and Technology University. The authors would like to thank the editors and reviewers for their suggestions to improve the quality of the manuscript.

References

[1] World Health Organization (WHO), *World Malaria Report*, Global Malaria Programme, Geneva, Switzerland, 2019. https://www.who.int/en/news-room/fact-sheets/detail/malaria.

[2] Coetzee, M., *Distribution of The African Malaria Vectors of The Anopheles Gambiae Complex*, Am. J. Trop. Med. Hyg., **70**, pp. 103-114, 204.

[3] Agusto, F.B., Gumel, A.B. & Parham, P.E., *Qualitative Assessment of The Role of Temperature Variations on Malaria Transmission Dynamics*, J. Biol. Sci., **23**, pp. 597-630, 2015.

[4] Okosun, K.O., Ouifki, R. & Marcus, N., *Optimal Control Analysis of a Malaria Transmission Model That Includes Treatment and Vaccination with Waning Immunity*, BioSystems, **106**, pp. 136-145, 2011.

[5] Ross, R., *The Prevention of Malaria*, John Murray, London, 1911.

[6] Traore, B., Koutou, O. & Sangare, B., *A Global Mathematical Model of Malaria Transmission Dynamics with Structured Mosquito Population and Temperature Variations*, Nonlinear Anal. Real World Appl., **53**, 103081, 2020.

[7] Nwankwo, A. & Okuonghae, D., *Mathematical Assessment of The Impact of Different Microclimate Conditions on Malaria Transmission*, Math. Biosci., **1**, pp. 1414-1444, 2019.

[8] Mohammed-Awel, J., Agusto, F., Mickens, R. & Gumel, A., *Mathematical Assessment of The Role of Vector Insecticide Resistance and Feeding Behavior on Malaria Transmission Dynamics: Optimal Control Analysis*, Infect. Dis. Model., **3**, pp. 301-321, 2018.

[9] Abiodun, G.J., Witbooi, P. & Okosun, K.O., *Mathematical Modelling and Analysis of Mosquitohuman Malaria Model*, Hacettepe J. Math. Stat., **47**, pp. 219-235, 2018.

[10] Okuneye, K., Eikenberry, S.E. & Gumel, A.B., *Weather-Driven Malaria Transmission Model with Gonotrophic and Sporogonic Cycles*, J. Biol. Dyn., **13**, pp. 288-324, 2019.

[11] Abiodun, G. J., Maharaj, R., Witbooi, P. & Okosun, K. O., *Modelling the Influence of Temperature and Rainfall on the Population Dynamics of Anopheles Arabiensis*, Malar J., **15**(1), pp. 364-381, 2016.

[12] Olaniyi, S., Okosun, K., Adesanya, S. & Lebelo, S., *Modelling Malaria Dynamics with Partial Immunity and Protected Travellers: Optimal Control and Cost-Effectiveness Analysis*, J. Biol. Dyn., **14**, pp. 90-115, 2020.

[13] Makinde, O.D. & Okosun, K.O., *Impact of Chemotherapy on Optimal Control of Malaria Disease with Infected Immigrants*, BioSystems, **104**, pp. 32-41, 2011.

[14] Okosun, K.O., Ouifki, R. & Marcus, N., *Optimal Control Strategies and Cost-Effectiveness Analysis of a Malaria Model*, BioSystems, **111**, pp. 83-101, 2013.

[15] Otieno, G., Koske, J. & Mutiso, J., *Transmission Dynamics and Optimal Control of Malaria in Kenya*, Discrete Dyn. Nat. Soc., **2016**, 2016.

[16] Gashaw, K.W., *Climate Dependent Malaria Disease Transmission Model and Its Analysis*, PhD dissertation, Department of mathematics, Addis Ababa University, Ethiopia, 2018.

[17] Sanchez, Y.G., Sabir Z. & Guirao, J.L., *Design of A Nonlinear SITR Fractal Model Based on The Dynamics of a Novel Coronavirus (COVID)*, Fractals, **28**(8), 2020.

[18] Umar, M., Sabir, Z., Raja, M.Z., Shoaib, M., Gupta M. & Sanchez, Y.G., *A Stochastic Intelligent Computing with Neuro-Evolution Heuristics for Nonlinear SITR System of Novel COVID-19 Dynamics*, Symmetry, **12**(10), 2020.

[19] Evirgen, F., Ucar, S. & Ozdemir, N., *System Analysis of HIV Infection Model with $CD4^{+}T$ under Non-Singular Kernel Derivative*, Applied Mathematics and Nonlinear Sciences, **5**(1), 139-146, 2020.

[20] Belgaid, Y., Helal, M. & Venturino, E., *Mathematical Analysis of a B-Cell Chronic Lymphocytic Leukemia Model with Immune Response*, Applied Mathematics and Nonlinear Sciences, **4**(2), pp. 551-558, 2019.

[21] Anda-Jáuregui, G. de, Fresno, García-Cortés, C., Enríquez, D., Espinal, J. & Hernández-Lemus, E., *Intrachromosomal Regulation Decay in Breast Cancer*, Applied Mathematics and Nonlinear Sciences, **4**(1), pp. 223-230, 2019.

[22] Okosun, K.O., Makinde, O.D. & Takaidza, I., *Impact of Optimal Control on The Treatment of HIV/AIDS and Screening of Unaware Infectives*, Appl. Math. Model., **37**, pp. 3802-3820, 2013.

[23] Fister, K.R., Lenhart, S. & McNally, J.S., *Optimizing Chemotherapy in an HIV Model*, Electron. J. Differ. Equ., 1998.

[24] Van den Driessche, P. & Watmough J., *Reproduction Numbers and Sub-Threshold Endemic Equilibria for Compartmental Models of Disease Transmission*, Math. Biosci., 180, pp. 29-48, 2002.

[25] Mojeeb, A., Osman, E. & Isaac, A.K., *Simple Mathematical Model for Malaria Transmission*, J. Adv. Math. Comput. Sci., **25**, pp. 1-24, 2017.

[26] Castillo-Chavez, C., Blower, S., Driessche, P., Kirschner, D. & Yakubu, A., *Mathematical Approaches for Emerging and Reemerging Infectious Diseases: Models, Methods, and Theory*, Springer Science and Business Media, **1**, 2002.

[27] LaSalle, J. P., *The Stability of Dynamical Systems, Society for Industrial and Applied Mathematics*, In Proceedings of the Conference Series in Applied Mathematics, **25**, 1976.

[28] Chitnis, N., Hyman, J.M. & Cushing, J.M., *Determining Important Parameters in the Spread of Malaria Through the Sensitivity Analysis of a Mathematical Model*, Bull. Math. Biol., **70**, pp. 1272-1296, 2008.

[29] Niger, A. & Gumel, B., *Mathematical Analysis of the Role of Repeated Exposure on Malaria Transmission Dynamics*, Differ. Equ. Dyn. Syst., **16,** pp. 251-87, 2008.

[30] Khan, M. A., Wahid, A., Islam, S., Khan, I., Shafie, S. & Gul, T., *Stability Analysis of An SEIR Epidemic Model with Non-Linear Saturated Incidence and Temporary Immunity*, Int. J. Adv. Appl. Math. and Mech., **2**, pp. 1-14, 2015.

[31] Temesgen, D.K., Makinde, O.D. & Legesse, O.L., *Modelling and Optimal Control Analysis of Malaria Epidemic in the Presence of Temperature Variability*, Asian European Journal of Mathematics, pp. 2250005, 2021.

[32] Agusto, F.B., Marcus N. & Okosun K.O, *Application of Optimal Control to the Epidemiology of Malaria*, Electron. J. Differ. Equ., **81**, pp. 1-22, 2012.

[33] Bhuju, G., Phaijoo, G.R. & Gurung, D.B., *Mathematical Study on Impact of Temperature in Malaria Disease Transmission Dynamics*, Adv. Comput. Sci., **1**(2), 2018.

[34] Lenhart S. & Workman, J.T., *Optimal Control Applied to Biological Models*, CRC Mathematical and Computational Biology Series, 2007.

[35] Van den Driessche, P. & Watmough J., *Reproduction Numbers and Sub-Threshold Endemic Equilibria for Compartmental Models of Disease Transmission*, Math. Biosci., **180**, pp. 29-48, 2002.

[36] Okosun, K.O., Mukamuri, M. & Makinde, O.D., *Global Stability Analysis and Control of Leptospirosis*, Open Math., **1**, pp. 567-585, 2016.

[37] Pontryagin, L.S., Boltyanskii, V.G., Gamkrelidze, R.V. & Mishchenko, E.F., *The Mathematical Theory of Optimal Processes*, Wiley, New York, 1962.

[38] Fleming W.H. & Rishel, R.W., *Deterministic and Stochastic Optimal Control*, Springer, New York, USA, **1**, 1975.

[39] Berhe, H. W, Makinde, O.D. & Malonza, D, *Co-dynamics of Measles and Dysentery Diarrhea Diseases with Optimal Control and Cost-effectiveness Analysis*, Applied Mathematics and Computation, **347**, 903-921, 2019.